ChemComm

COMMUNICATION

View Article Online
View Journal | View Issue

Cite this: *Chem. Commun.*, 2015, 51, 8082

Received 5th March 2015,
Accepted 1st April 2015

DOI: 10.1039/c5cc01885d

www.rsc.org/chemcomm

Singlet oxygen generation from $Li^+@C_{60}$ nano-aggregates dispersed by laser irradiation in aqueous solution†

Kei Ohkubo,*[a] Naoki Kohno,[a] Yusuke Yamada[a] and Shunichi Fukuzumi*[abc]

Laser pulse irradiation of a deaerated aqueous solution containing the solid state lithium ion-encapsulated fullerene resulted in the formation of highly dispersed nano-aggregates $(Li^+@C_{60})_n$. Photoirradiation of an O_2-saturated D_2O solution containing $(Li^+@C_{60})_n$ gave singlet oxygen with 55% quantum yield, leading to efficient double-stranded DNA cleavage.

Photodynamic therapy (PDT) has developed as a non-invasive clinical treatment of various dermatological, ophthalmic and cardiovascular diseases.[1–6] The tumour cell apoptosis in the PDT treatment is carried out by photoirradiation of the photosensitiser to generate the reactive oxygen species (ROS) such as singlet oxygen ($^1O_2$*) and superoxide ($O_2^{\bullet-}$) in malignant tumour.[1–6] The requirements of an ideal photosensitiser are water solubility, low cytotoxicity in the dark, high stability against light, high tumour-specificity, high ability to produce ROS and rapid metabolism.[1–6]

Fullerenes, especially [60]fullerene (C_{60}), are known as efficient photosensitisers to generate the triplet excited state and ROS with high quantum yields ($\Phi(^3C_{60}$*) = 0.98; $\Phi(^1O_2$*) = 0.96 in C_6D_6).[7] Additionally, fullerenes are remarkably photostable and non-toxic reagents.[8] However, pristine C_{60} is hardly soluble in water (0.4 μg mL^{-1} at 298 K)[9] and biological media to prevent expression of the photoactivity and PDT efficiency.[10,11] Therefore, various fullerene derivatives, such as C_{60} with polyethyleneglycol,[12] and γ-cyclodextrin-,[13–15] lipid-membrane-[16] and porous silicate-incorporated C_{60},[17] have been reported to improve water solubility.[18] Introduction of water-soluble substituents has also been reported; however, molecular C_{60} and substituted C_{60} have no strong absorption around 600–800 nm. Fullerene dispersion suspended in water is also reported by reprecipitation, solvent replacement, ultrasonication and laser ablation methods.[19–22]

Recently, a lithium ion-encapsulated fullerene hexafluorophosphate salt ($Li^+@C_{60}$ PF_6^-) has been reported as an efficient photosensitiser to form the long-lived triplet excited state, which is comparable to that of C_{60}.[23] However, neither solubilisation of $Li^+@C_{60}$, C_{60} or C_{70} in water nor the photoinduced singlet oxygen generation efficiency has been studied. We report herein highly water-dispersed heterogeneous fullerene nano-aggregates composed of $Li^+@C_{60}$, C_{60}, and C_{70}, which have absorption bands in the visible region as well as an efficient singlet oxygen generation properties.

The solubility of the $Li^+@C_{60}PF_6^-$ salt is extremely low in water as shown in the inset pictures in Fig. 1a, where the black powders are deposited at the bottom of the cuvette. Laser pulse irradiation (λ = 532 nm; 500 mW; 10 Hz, 60 min, i.d. = 8 mm) of a deaerated aqueous solution (2.5 mL) containing the dispersed $Li^+@C_{60}PF_6^-$ salt (1.0 mg) resulted in the formation of $Li^+@C_{60}$ nano-aggregates $[(Li^+@C_{60})_n]$. A brown colour supernatant solution containing nano-aggregates was obtained after the centrifugation (15 000 rpm for 10 min) and decantation procedures. The UV-vis absorption spectra of nano-aggregates in water are shown in Fig. 1, exhibiting two characteristic absorption bands for $(Li^+@C_{60})_n$ in water at 264 and 340 nm, which are red-shifted as compared to that in a dichloromethane solution (257 and 327 nm) by aggregation. A broad shoulder absorption band is also shown at around 400–600 nm, which is characteristic of an intermolecular charge-transfer (CT) transition between fullerenes in the nano-aggregates. A similar CT band was observed for $(C_{60})_n$. Such a CT band has been reported in the case of a C_{60} thin film.[24] The enhancement of solubility of $(Li^+@C_{60})_n$ and $(C_{60})_n$ in water may be obtained by CT interactions.[25] The solubilisation of C_{60} aggregates may occur without the substitution and decomposition of the fullerene cages, which was confirmed by MALDI-TOF-MS spectral measurements indicating the only peak due to non-substituted fullerene.

[a] *Department of Material and Life Science, Graduate School of Engineering, Osaka University, ALCA and SENTAN, Japan Science and Technology Agency (JST), Suita, Osaka 565-0871, Japan. E-mail: ookubo@chem.eng.osaka-u.ac.jp, fukuzumi@chem.eng.osaka-u.ac.jp*
[b] *Department of Bioinspired Science, Ewha Womans University, Seoul 120-750, Korea*
[c] *Faculty of Science and Engineering, Meijo University, ALCA and SENTAN, Japan Science and Technology Agency (JST), Nagoya, Aichi 468-0073, Japan*

† Electronic supplementary information (ESI) available: Experimental and spectroscopic details. See DOI: 10.1039/c5cc01885d

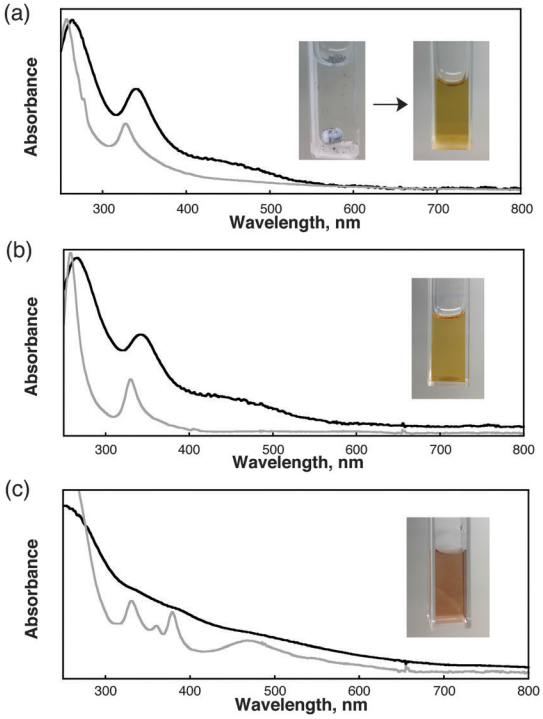

Fig. 1 Electronic absorption spectra of (a) $(Li^+@C_{60})_n$, (b) $(C_{60})_n$ and (c) $(C_{70})_n$ dispersed in distilled water at 298 K. Inset: pictures of $(Li^+@C_{60})_n$ before and after laser light irradiation for 60 min and centrifugation. Absorption spectra in dichloromethane solutions are shown as grey lines.

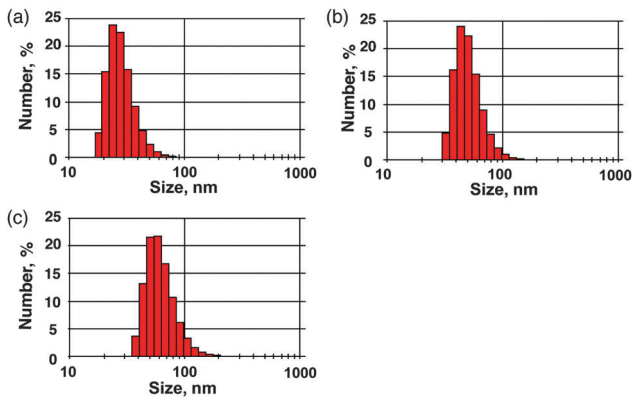

Fig. 2 Particle size distributions determined by dynamic light scattering (DLS) of (a) $(Li^+@C_{60})_n$, (b) $(C_{60})_n$ and (c) $(C_{70})_n$.

The dynamic light scattering (DLS) measurements were performed to evaluate the size of $(Li^+@C_{60})_n$ as shown in Fig. 2. The size of the nano-aggregates was significantly decreased to 30 nm by the laser pulse excitations. Thus, one nano-aggregate consists of *ca.* 30 000 $Li^+@C_{60}$ molecules. When $Li^+@C_{60}PF_6^-$ was replaced by C_{60} and C_{70}, the highly dispersed nano-aggregates were also obtained by laser pulse irradiation. The sizes of C_{60} and C_{70} nano-aggregates were estimated to be 52 and 64 nm, which are larger than $(Li^+@C_{60})_n$. Transmission electron microscopy (TEM) measurements of $(Li^+@C_{60})_n$ were performed to evaluate the formation of nano-aggregates, indicating the grape bunch morphology of the nano-aggregates of 30–40 nm size (Fig. 3).

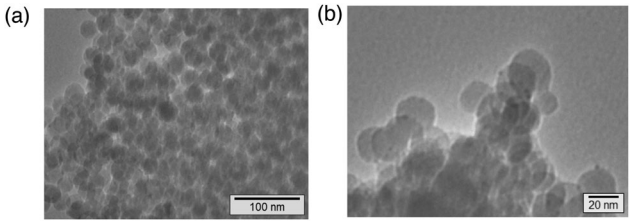

Fig. 3 TEM images of $(Li^+@C_{60})_n$. (a) Large scale and (b) detailed views.

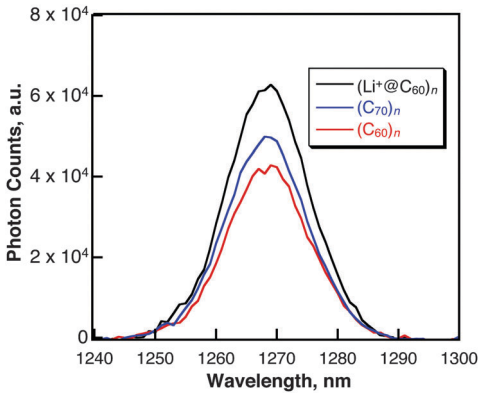

Fig. 4 Emission spectra of $^1O_2$ obtained by photoirradiation (λ = 532 nm) of O_2-saturated D_2O solutions containing $(Li^+@C_{60})_n$, $(C_{60})_n$ and $(C_{70})_n$ at 298 K.

Table 1 Quantum yields of singlet oxygen of molecular fullerene and their nano-aggregates

Fullerene	Φ^a	Fullerne aggregates	Φ^b
$Li^+@C_{60}$	0.83	$(Li^+@C_{60})_n$	0.55
C_{60}	0.96[c]	$(C_{60})_n$	0.30
C_{70}	0.81[c]	$(C_{70})_n$	0.41

[a] Dissolved in C_6D_6/C_6H_5CN (1 : 1 v/v). Emission data are shown in Fig. S1 in the ESI. [b] Dispersed in D_2O. [c] Taken from ref. 6.

The $(Li^+@C_{60})_n$ solution was stable at room temperature for three days without re-aggregation.

Photoirradiation of an oxygen-saturated deuterated water (D_2O) solution of $(Li^+@C_{60})_n$ results in the formation of singlet oxygen, which was detected by $^1O_2$ phosphorescence at 1270 nm (Fig. 4).[4] The quantum yields (Φ) of $^1O_2$ generation were determined from the phosphorescence intensity, which was compared to the intensity obtained using rose bengal as a reference compound (Φ = 0.77).[26] Relatively high Φ values are obtained and the values are summarised in Table 1, in which the highest Φ value is 0.55 for $(Li^+@C_{60})_n$. The values of nano-aggregates are smaller than those of the corresponding fullerenes in C_6D_6/C_6H_5CN (1 : 1 v/v) probably because of excited state annihilation (*vide infra*).

Femtosecond and nanosecond time-resolved transient absorption spectral measurements were performed to clarify the excited state dynamics and reaction mechanisms for the formation of singlet oxygen from $(Li^+@C_{60})_n$. Ultrafast photodynamics for intersystem crossing (ISC) from the singlet to the triplet excited state of $(Li^+@C_{60})_n$ was observed by femtosecond

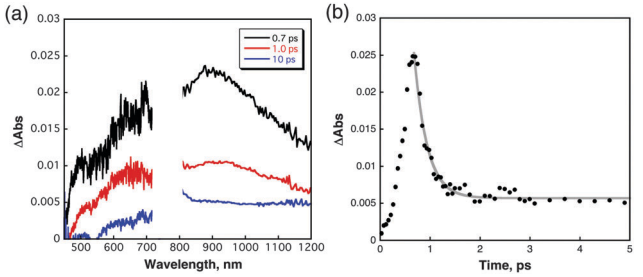

Fig. 5 (a) Transient absorption spectra of $(Li^+@C_{60})_n$ in deaerated distilled water obtained by femtosecond laser excitation at 393 nm. (b) Decay time profile at 900 nm with a single-exponential decay curve.

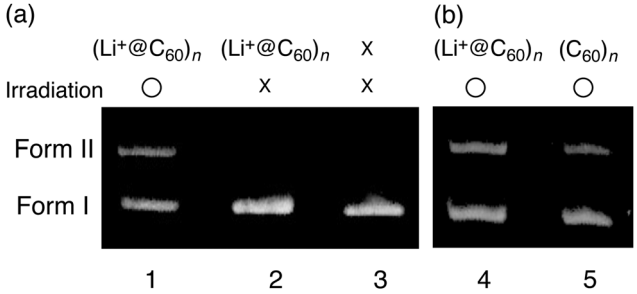

Fig. 6 Agarose gel electrophoresis of photoinduced cleavage of supercoiled pBR322 DNA (0.051 mg mL^{-1}) (a) (lane 1) with $(Li^+@C_{60})_n$ after photoirradiation (lane 2) with $(Li^+@C_{60})_n$ stored in the dark and (lane 3) without $(Li^+@C_{60})_n$ (b) (lane 4) with $(Li^+@C_{60})_n$ and (lane 5) $(C_{60})_n$ in O_2-saturated buffer solutions (pH 8.2).

laser flash photolysis. The transient absorption band at 960 nm taken at 10 ps after the femtosecond laser pulse excitation at 393 nm is assigned to the singlet excited state of $Li^+@C_{60}$ [$^1(Li^+@C_{60})^*$] in nano-aggregates (Fig. 5), which is relatively broadened as compared to the singlet–singlet absorption of $Li^+@C_{60}$ in PhCN.[27] The decay of absorbance at 900 nm obeyed a two-exponential curve. The faster component could be assigned to the singlet–singlet annihilation in the $(Li^+@C_{60})_n$ nano-aggregates because the ratio of the faster component increased with increasing the excitation laser power intensity without changing the rate constant (3.8×10^{12} s^{-1}) (Fig. S2 in the ESI†). The residual absorption band at 900 nm slowly decayed with the appearance of the absorption band at 700 nm due to the triplet excited state of the $Li^+@C_{60}$ dimer.[28] The decay rate constant of the slower part was determined to be 6.6×10^8 s^{-1}, which is virtually the same as that of the formation of the triplet excited state of $Li^+@C_{60}$ (7.0×10^8 s^{-1}) (see Fig. S3 in the ESI†). This value is slightly slower than the value of homogeneous $Li^+@C_{60}$ in PhCN (8.9×10^8 s^{-1}).[27]

The triplet excited state of $(Li^+@C_{60})_n$ is also detected by the transient absorption spectral measurements observed in a strictly deaerated aqueous solution after nanosecond laser excitation at 355 nm. The transient absorption band taken at 20 ns are due to the triplet–triplet (T–T) transition (see Fig. S3a in ESI†). The band is significantly broadened compared to the case of $Li^+@C_{60}$ in PhCN. The T–T absorption maximum of $(Li^+@C_{60})_n$ is virtually the same as that of $Li^+@C_{60}$ (λ_{max} = 750 nm).[27] This suggests the aggregation with strong π stacking between the fullerene cages in $(Li^+@C_{60})_n$. The decay of T–T absorption obeyed the first-order kinetics. The lifetime of the transient species was determined to be 32 ns (Fig. S4 in the ESI†). There was no contribution of the T–T annihilation, because the triplet lifetime remained constant at different laser power intensities (Fig. S4b in ESI†). The short triplet lifetime may result from the strong π stacking between the fullerene cages in $(Li^+@C_{60})_n$. On the other hand, no T–T absorption spectrum was observed when $(Li^+@C_{60})_n$ was replaced by $(C_{60})_n$ and $(C_{60})_n$ under otherwise the same experimental conditions.[28] The π stacking in $(Li^+@C_{60})_n$ is much weaker than those of $(C_{60})_n$ and $(C_{60})_n$ because $(Li^+@C_{60})_n$ contains equivalent number of PF_6^- counter anions in the nano-aggregates to avoid π–π interaction between the fullerene cages.[29]

The triplet excited state of $(Li^+@C_{60})_n$ can be an active species for formation of singlet oxygen by energy transfer with molecular O_2. We also examined the DNA-cleavage activity of $(Li^+@C_{60})_n$ in the presence of O_2 using the widely used assay with the supercoiled double-stranded plasmid DNA, pBR322, because singlet oxygen is formed by the photoirradiation of $(Li^+@C_{60})_n$ in aqueous solution. The agarose gel electrophoresis was performed after 10 h photoirradiation of pBR 322 with a xenon lamp ($\lambda >$ 380 nm) in the presence of $(Li^+@C_{60})_n$ in comparison with the control experiments as shown in Fig. 6a. Photoirradiation of $(Li^+@C_{60})_n$ in the presence of O_2 is significantly effective for DNA cleavage due to the singlet oxygen generation due to the observation of a large amount of cleaved DNA (Form II). The DNA cleavage activity of $(Li^+@C_{60})_n$ is much higher than that of $(C_{60})_n$ as shown in Fig. 6b, suggesting that a cationic $(Li^+@C_{60})_n$ may electrostatically access the minor grove in the double-stranded DNA.

In conclusion, highly dispersed $(Li^+@C_{60})_n$ produced by laser irradiation of $Li^+@C_{60}$ acts as an efficient photosensitiser for generation of singlet oxygen in aqueous solution. The excited states of $(Li^+@C_{60})_n$ have been successfully detected by femto- and nanosecond transient absorption spectroscopies. We believe that water-soluble $(Li^+@C_{60})_n$ can be employed as a convenient PDT photosensitiser in the near future.

This work was supported by Grants-in-Aid (no. 26620154 and 26288037 to K.O. and no. 24350069 and 25600025 to Y.Y.) from the Ministry of Education, Culture, Sports, Science and Technology (MEXT); ALCA and SENTAN projects from JST, Japan (to S.F.). We acknowledge Research Centre for Ultra-Precision Science & Technology in Osaka University for TEM measurements.

Notes and references

1 R. Bonnett, *Chemical Aspects of Photodynamic Therapy*, Gordon and Breach Science Publishers, Amsterdam, 2000.
2 M. Hurtgen, A. Debuigne, M. Hoebecke, C. Passirani, N. Lautram, A. Mouithys-Mickalad, P.-H. Guelluy, C. Jérome and C. Detrembleur, *Macromol. Biosci.*, 2013, **13**, 106–115.
3 K. Lang, J. Mosinger and D. M. Wagnerova, *Coord. Chem. Rev.*, 2004, **248**, 321–350.
4 (*a*) S. Gross, A. Gilead, A. Scherz, M. Neeman and Y. Salomon, *Nat. Med.*, 2003, **9**, 1327–1331; (*b*) D. E. J. G. J. Dolmans, D. Fukumura and R. K. Jain, *Nat. Rev. Cancer*, 2003, **3**, 380–387.
5 (*a*) Y.-Y. Huang, S. K. Sharma, R. Yin, T. Agrawal, L. Y. Chiang and M. R. Hamblin, *J. Biomed. Nanotechnol.*, 2014, **10**, 1918–1936; (*b*) Q. Li, H. Ruan and H. Li, *Pharm. Nanotechnol.*, 2014, **2**, 25–64.

6 (*a*) T. J. Dougherty, C. J. Gomer, B. W. Henderson, G. Jori, D. Kessel, M. Korbelik, J. Moan and Q. Peng, *J. Natl. Cancer Inst.*, 1998, **90**, 889–905; (*b*) W. M. Sharman, C. M. Allen and J. E. van Lier, *Drug Discovery Today*, 1999, **4**, 507–517.
7 (*a*) J. W. Arbogast, A. P. Darmanyan, C. S. Foote, F. N. Diederich, Y. Rubin, M. M. Alvarez, S. J. Anz and R. L. Whetten, *J. Phys. Chem.*, 1991, **95**, 11–12; (*b*) J. W. Arbogast and C. S. Foote, *J. Am. Chem. Soc.*, 1991, **113**, 8886–8889.
8 (*a*) M. Wang, L. Huang, S. K. Sharma, S. Jeon, S. Thota, F. F. Sperandio, S. Nayka, J. Chang, M. R. Hamblin and L. Y. Chiang, *J. Med. Chem.*, 2012, **55**, 4274–4285; (*b*) N. Gharbi, M. Pressac, M. Hadchouel, H. Szwarc, S. R. Wilson and F. Moussa, *Nano Lett.*, 2005, **5**, 2578–2585.
9 (*a*) D. Heymann, *Fullerene Sci. Technol.*, 1996, **4**, 509–515; (*b*) Y. Marcus, A. L. Smith, M. V. Korobov, A. L. Mirakyan, N. V. Avramenko and E. B. Stukalin, *J. Phys. Chem. B*, 2001, **105**, 2499–2506.
10 S. K. Sharma, L. Y. Chiang and M. R. Hamblin, *Nanomedicine*, 2011, **6**, 1813–1825.
11 P. Mroz, G. P. Tegos, H. Gali, T. Wharton, T. Sarna and M. R. Hamblin, *Photochem. Photobiol. Sci.*, 2007, **6**, 1139–1149.
12 (*a*) T. Andersson, K. Nilsson, M. Sundahl, G. Westman and O. Wennerström, *J. Chem. Soc., Chem. Commun.*, 1992, 604–606; (*b*) K. Komatsu, K. Fujiwara, Y. Murata and T. Braun, *J. Chem. Soc., Perkin Trans. 1*, 1999, 2963–2966.
13 Y. Yamakoshi, S. Aoua, T.-M. D. Nguyen, Y. Iwamoto and T. Ohnishi, *Faraday Discuss.*, 2014, **173**, 287–296.
14 W. Zhang, X. Gong, C. Liu, Y. Piao, Y. Sun and G. Diao, *J. Mater. Chem. B*, 2014, **2**, 5107–5115.
15 I. Nakanishi, S. Fukuzumi, T. Konishi, K. Ohkubo, M. Fujitsuka, O. Ito and N. Miyata, *J. Phys. Chem. B*, 2002, **106**, 2372–2380.
16 A. Ikeda, Y. Doi, M. Hashizume, J.-i. Kikuchi and T. Konishi, *J. Am. Chem. Soc.*, 2007, **129**, 4140–4141.
17 S.-R. Chae, A. R. Badireddy, J. F. Budarz, S. Lin, Y. Xiao, M. Therezien and M. R. Wiesner, *ACS Nano*, 2010, **4**, 5011–5018.
18 (*a*) T. D. Ros and M. Prato, *Chem. Commun.*, 1999, 663–669; (*b*) E. Nakamura and H. Isobe, *Acc. Chem. Res.*, 2003, **36**, 807–815.
19 G. V. Andrievsky, M. V. Kosevich, O. M. Vovk, V. S. Shelkovsky and L. A. Vashchenko, *J. Chem. Soc., Chem. Commun.*, 1995, 1281–1282.
20 S. Deguchi, R. G. Alargova and K. Tsujii, *Langmuir*, 2001, **17**, 6013–6017.
21 W.-B. Ko, J.-Y. Heo, J.-H. Nam and K.-B. Lee, *Ultrasonics*, 2004, **41**, 727–730.
22 (*a*) T. Asahi, T. Sugiyama and H. Masuhara, *Acc. Chem. Res.*, 2008, **41**, 1790–1798; (*b*) T. Sugiyama, S.-i. Ryo, I. Oh, T. Asahi and H. Masuhara, *J. Photochem. Photobiol., A*, 2009, **207**, 7–12; (*c*) H. Tabata, M. Akamatsu, M. Fujii and S. Hayashi, *Jpn. J. Appl. Phys.*, 2007, **46**, 4338–4343.
23 Y. Kawashima, K. Ohkubo and S. Fukuzumi, *Chem. – Asian J.*, 2015, **10**, 44–54.
24 S. Kazaoui, R. Ross and N. Minami, *Solid State Commun.*, 1994, **90**, 623–628.
25 Enhancement of solubility by charge-transfer formation: see (*a*) A. P. O'Mullane, N. Fay, A. Nafady and A. M. Bond, *J. Am. Chem. Soc.*, 2007, **129**, 2066–2073; (*b*) I. Natori, S. Natori and K. Ogino, *Macromolecules*, 2009, **42**, 1964–1969; (*c*) H. Destaillats and R. Fernández-Prini, *J. Chem. Soc., Faraday Trans.*, 1998, **94**, 871–878.
26 R. W. Redmond and J. N. Gamlin, *Photochem. Photobiol.*, 1999, **70**, 391–475.
27 (*a*) Y. Kawashima, K. Ohkubo and S. Fukuzumi, *J. Phys. Chem. A*, 2012, **116**, 8942–8948; (*b*) K. Ohkubo, Y. Kawashima and S. Fukuzumi, *Chem. Commun.*, 2012, **48**, 4314–4316.
28 Y. Ishibashi, M. Arinishi, T. Katayama, H. Miyasaka and T. Asahi, *Chem. Lett.*, 2012, **41**, 1104–1106.
29 Solid state $Li^{+}@C_{60}$ PF_6^{-} is known to be a rock-salt type crystal structure. see: S. Aoyagi, Y. Sado, E. Nishibori, H. Sawa, H. Okada, H. Tobita, Y. Kasama, R. Kitaura and H. Shinohara, *Angew. Chem., Int. Ed.*, 2012, **51**, 3377–3381.